THE JOURNAL OF BIOLOGICAL CHEMISTRY VOL. 288, NO. 28, pp. 20306–20314, July 12, 2013

Discrete Control of TRPV4 Channel Function in the Distal Nephron by Protein Kinases A and C*

Received for publication, March 5, 2013, and in revised form, May 6, 2013 Published, JBC Papers in Press, May 24, 2013, DOI 10.1074/jbc.M113.466797

Mykola Mamenko, Oleg L. Zaika, Nabila Boukelmoune, Jonathan Berrout, Roger G. O'Neil, and Oleh Pochynyuk[1]

From the Department of Integrative Biology and Pharmacology, The University of Texas Health Science Center at Houston, Houston, Texas 77030

Background: TRPV4 mediates flow-induced $[Ca^{2+}]_i$ responses in distal nephron cells.
Results: Activation of PKC augments TRPV4-mediated responses to flow. Activation of PKA promotes TRPV4 translocation to the apical membrane.
Conclusion: TRPV4 activity and TRPV4 trafficking are under discrete but synergistic control of PKC- and PKA-dependent pathways.
Significance: Systemic physiological stimuli may affect TRPV4-mediated mechanosensitivity in the distal nephron via PKA- and PKC-dependent mechanisms.

We have recently documented that the Ca^{2+}-permeable TRPV4 channel, which is abundantly expressed in distal nephron cells, mediates cellular Ca^{2+} responses to elevated luminal flow. In this study, we combined Fura-2-based $[Ca^{2+}]_i$ imaging with immunofluorescence microscopy in isolated split-opened distal nephrons of C57BL/6 mice to probe the molecular determinants of TRPV4 activity and subcellular distribution. We found that activation of the PKC pathway with phorbol 12-myristate 13-acetate significantly increased $[Ca^{2+}]_i$ responses to flow without affecting the subcellular distribution of TRPV4. Inhibition of PKC with bisindolylmaleimide I diminished cellular responses to elevated flow. In contrast, activation of the PKA pathway with forskolin did not affect TRPV4-mediated $[Ca^{2+}]_i$ responses to flow but markedly shifted the subcellular distribution of the channel toward the apical membrane. These actions were blocked with the specific PKA inhibitor H-89. Concomitant activation of the PKA and PKC cascades additively enhanced the amplitude of flow-induced $[Ca^{2+}]_i$ responses and greatly increased basal $[Ca^{2+}]_i$ levels, indicating constitutive TRPV4 activation. This effect was precluded by the selective TRPV4 antagonist HC-067047. Therefore, the functional status of the TRPV4 channel in the distal nephron is regulated by two distinct signaling pathways. Although the PKA-dependent cascade promotes TRPV4 trafficking and translocation to the apical membrane, the PKC-dependent pathway increases the activity of the channel on the plasma membrane.

The transient receptor potential (TRP)[2] superfamily is an association of six-transmembrane domain cation channels with a remarkable diversity of gating properties, selectivity, and specific activation mechanisms (1). TRP channels are widely expressed in both excitable and non-excitable cells (2). Due to activation in response to a broad range of stimuli, including chemical compounds, temperature, mechanical inputs, etc., TRP channels are viewed as essential components in virtually all cellular responses to dynamic environmental changes (1, 2). TRP channel dysfunction has been recently linked to a number of hereditary diseases in humans ranging from skeletal dysplasias, neuropathies, and electrolyte imbalance (magnesemia and hypocalcemia) to polycystic kidney disease (3–7).

TRPV4 (TRP subfamily V member 4) is a relatively nonselective Ca^{2+}-permeable channel with prominent expression in many organs, including the kidney (reviewed in Ref. 8). TRPV4 is known to be activated by mechanical stress, including hypotonicity and shear stress arising from elevated fluid flow (8–10). Interestingly, TRPV4 expression in the renal nephron appears to be restricted to the distal segments, including the collecting duct and the connecting tubule, which are particularly subjected to variations of fluid flow and composition (11). This pattern of TRPV4 activation is consistent with a recently proposed role of the channel in mediating mechanosensitive elevations in $[Ca^{2+}]_i$ in renal tubular cells (11). Indeed, our group recently demonstrated that genetic ablation of TRPV4 abolishes flow-dependent $[Ca^{2+}]_i$ responses in microdissected distal nephron preparations (12). Consistently, flow-dependent K^+ secretion in the distal nephron, a Ca^{2+}-dependent process utilizing the maxi-K channel (13, 14), is absent in TRPV4 knock-out animals (15).

Several reports have demonstrated that TRPV4 can physically interact with TRPP2 (also known as polycystin-2) in distal nephron cells to form mechanosensitive heteromeric complexes (16, 17). TRPV4 activity is drastically impaired in cyst cells from PCK453 rats, an animal model of autosomal recessive polycystic kidney disease (ARPKD), which is causative for the inability to increase $[Ca^{2+}]_i$ in response to elevated flow (18). Importantly, pharmacological stimulation of TRPV4 with GSK1016790A restores mechanosensitive $[Ca^{2+}]_i$ signaling and retards renal cystogenesis in ARPKD, suggesting potential therapeutic benefits in treatment of the disease (18).

* This work was supported, in whole or in part, by National Institutes of Health Grant DK095029 from NIDDK (to O. P.). This work was also supported by an S&R Foundation Ryuji Ueno award (to O. P.).
[1] To whom correspondence should be addressed: Dept. of Integrative Biology and Pharmacology, The University of Texas Health Science Center at Houston, 6431 Fannin, Houston, TX 77030. Tel.: 713-500-7466; Fax: 713-500-7455; E-mail: oleh.m.pochynyuk@uth.tmc.edu.
[2] The abbreviations used are: TRP, transient receptor potential; ARPKD, autosomal recessive polycystic kidney disease; PMA, phorbol 12-myristate 13-acetate; BIM-I, bisindolylmaleimide I.

Little is known about intracellular signaling mechanisms controlling TRPV4 function and, consequently, flow-mediated $[Ca^{2+}]_i$ elevations in the renal tubule. Recent evidence suggested that cGMP can act through PKG to inhibit flow-induced increases in $[Ca^{2+}]_i$ in cultured M1 collecting duct cells (17). However, the cGMP/PKG pathway has no direct inhibitory actions on TRPV4, but it acts on its heteromeric counterpart, TRPP2 (17). In contrast, experimental evidence in expression systems indicates that intracellular N and C termini of TRPV4 can be subjected to direct phosphorylation by PKC and PKA, resulting in augmentation of cellular responses to mechanical stress elicited by hypotonicity (19). However, it is unclear whether PKC and PKA play a role in regulation of TRPV4-mediated mechanosensitivity in the mammalian distal nephron.

In this study, we monitored subcellular TRPV4 distribution with immunofluorescence microscopy and assessed flow-induced $[Ca^{2+}]_i$ elevations as a physiologically relevant readout of the channel activity to probe the mechanism of TRPV4 regulation by PKC and PKA in freshly isolated split-opened distal nephrons. We found that the functional status of the TRPV4 channel in the distal nephron is regulated by two distinct signaling pathways. Although the PKA-dependent pathway appears to be responsible for TRPV4 trafficking and translocation to the apical membrane, the PKC-dependent pathway stimulates the activity of the channel on the plasma membrane.

EXPERIMENTAL PROCEDURES

Materials and Animals—All chemicals and materials were from Sigma, VWR International (Radnor, PA), and Tocris Bioscience (Ellisville, MO) unless noted otherwise and were reagent grade. Animal use and welfare adhered to the National Institutes of Health Guide for the Care and Use of Laboratory Animals following a protocol reviewed and approved by the Institutional Laboratory Animal Care and Use Committee of The University of Texas Health Science Center at Houston. For experiments, 6–8-week-old C57BL/6 mice (Charles Rivers Laboratories, Wilmington, MA) were used. Animals were maintained on standard rodent regimen (Purina 5001) and had free access to tap water.

Tissue Isolation—The procedure for isolation of the collecting ducts and the connecting tubules from C57BL/6 mice suitable for Ca^{2+} imaging and immunofluorescence microscopy closely follows the protocols reported previously by us (20–23). Kidneys were cut into thin slices (<1 mm) and placed into an ice-cold bath solution buffered with HEPES (pH 7.4). Distal nephrons were visually identified by their morphological features (pale color, coarse surface, and, in some cases, bifurcations) and were mechanically isolated from kidney slices by microdissection using watchmaker forceps under a stereomicroscope. Isolated distal nephrons were attached to 5 × 5-mm cover glasses coated with poly-L-lysine. A cover glass containing a distal nephron was placed in a perfusion chamber mounted on a Nikon Eclipse Ti inverted microscope and perfused with bath solution at room temperature. Distal nephrons were split open with two sharpened micropipettes, controlled with different micromanipulators, to gain access to the apical membrane. The nephrons were used within 1–2 h of isolation.

$[Ca^{2+}]_i$ Measurements—Intracellular calcium levels were measured in individual cells within the split-opened area of distal nephrons using Fura-2 fluorescence ratiometric imaging as described previously (20–23). Briefly, split-opened distal nephrons were loaded with Fura-2 by incubation with 2 μM Fura-2/AM in bath solution for 45 min at room temperature. Subsequently, tissue samples were washed and incubated for an additional 10–15 min prior to experimentation. Distal nephrons were then placed in an open-top imaging study chamber (Warner RC-10) with a bottom coverslip-viewing window, and the chamber was attached to the microscope stage of an InCa imaging workstation (Intracellular Imaging, Inc.). Cells were imaged with a 20× Nikon Super Fluor objective, and regions of interest were drawn for individual cells. The Fura-2 fluorescence intensity ratio was determined by excitation (an average for ~300 ms) at 340 and 380 nm and calculating the ratio of the emission intensities at 511 nm in the usual manner every 5 s. We observed no significant Fura-2 bleaching and minimal Fura-2 leakage at both wavelengths during experiments. The changes in the ratio were converted to intracellular Ca^{2+} concentrations using the calibration methods we have used before (12, 20, 22). At least three individual distal nephrons from three mice were used for each experimental set.

Immunofluorescence Microscopy—Freshly isolated and split-opened distal nephrons were fixed with 4% paraformaldehyde in PBS (pH 7.4) for 15 min at room temperature. After fixation, the samples were permeabilized by the addition of 0.1% Triton X-100 in PBS for 5 min and washed three times with PBS for 5 min. Nonspecific staining was blocked with 10% normal goat serum (Jackson ImmunoResearch Laboratories) in PBS for 30 min at room temperature. After washing three times with PBS for 5 min, the samples were incubated for 3 h at room temperature in the dark with anti-TRPV4 antibody (1:1000 dilution; Alomone Labs) in 1% normal goat serum and 0.1% Triton X-100 in PBS. Subsequently, the samples were washed three times with PBS and incubated for 1.5 h at room temperature in the dark with goat anti-rabbit IgG labeled with Alexa Fluor 488 (1:1000 dilution; Invitrogen) in 1% normal goat serum and 0.1% Triton X-100 in PBS. After washing three times with PBS for 5 min, the samples were stained with DAPI (1.5 μM; Calbiochem) to visualize nuclei. Subsequently, the samples were dehydrated and mounted with permanent mounting medium (Thermo Scientific). Labeled tissue samples were examined with an Nikon Eclipse Ti inverted confocal fluorescence microscope using a 40× Plan Fluor oil immersion (1.3 numerical aperture) objective. Samples were excited with 405 and 488 nm laser diodes, and emission was captured with a 16-bit CoolSNAP HQ^2 camera (Photometrics) interfaced to a PC running NIS-Elements version 4.00 software. Three-dimensional stacks of split-opened distal nephrons were generated from a series of confocal plane images with 0.25-μm steps.

Solutions—The typical bath solution was 150 mM NaCl, 5 mM KCl, 1 mM $CaCl_2$, 2 mM $MgCl_2$, 5 mM glucose, and 10 mM HEPES (pH 7.4). All reagents were applied by perfusing the experimental chamber at 1.5 ml/min. To test the effect of elevated flow on $[Ca^{2+}]_i$, the rate of perfusion was instantly increased from 1.5 ml/min (~15 mm H_2O) to 15 ml/min (~80 mm H_2O). Using a parallel plate chamber, we recently esti-

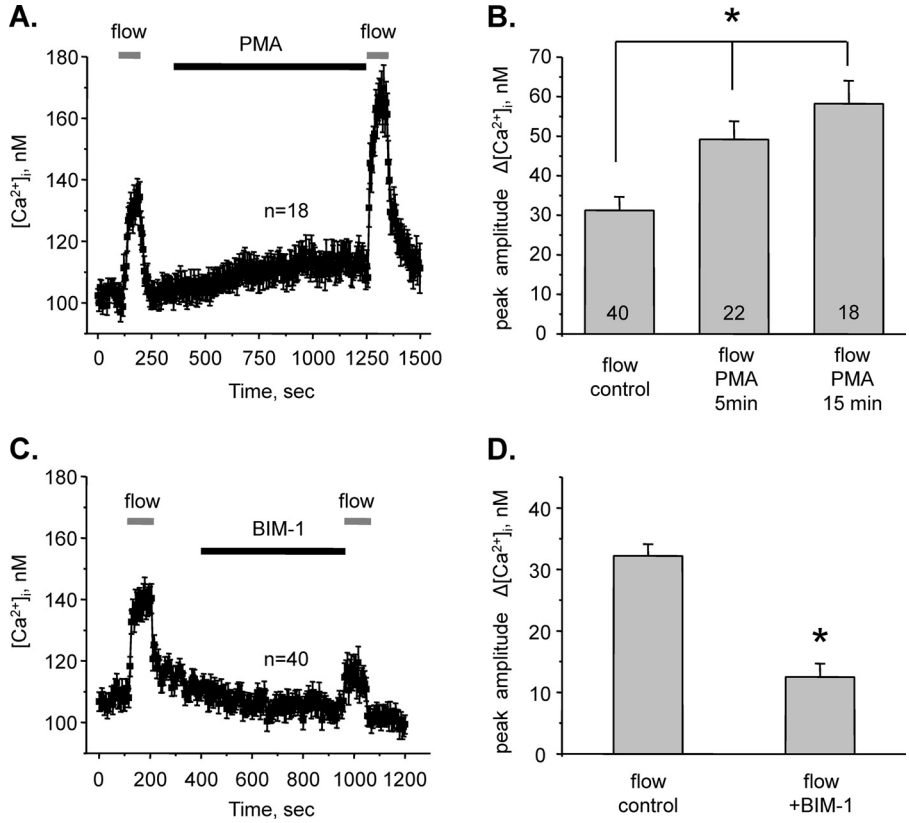

FIGURE 1. **PKC-dependent pathway modulates flow-dependent $[Ca^{2+}]_i$ elevations in distal nephron cells.** *A*, average time course of changes in $[Ca^{2+}]_i$ levels in response to 10-fold elevations in flow over the apical surface (*gray bars*) for individual distal nephron cells in the control and after treatment with the PKC activator PMA (200 nM; *black bar*). *B*, summary graph of the amplitude of $[Ca^{2+}]_i$ responses to flow in the control and after 5- and 15-min treatments with PMA. Here and below, the peak amplitude of $\Delta[Ca^{2+}]_i$ was calculated as the difference between the maximal $[Ca^{2+}]_i$ after flow increase and the average basal $[Ca^{2+}]_i$ level preceding the respective flow stimulus. *, significant increase *versus* flow control ($p < 0.01$ and $p < 0.001$ for 5 and 15 min of PMA treatment, respectively). *C*, average time course of changes in $[Ca^{2+}]_i$ levels in response to 10-fold elevations in flow over the apical surface (*gray bars*) for individual distal nephron cells in the control and after treatment with the PKC inhibitor BIM-I (200 nM; *black bar*). *D*, summary graph of the flow-induced changes in $[Ca^{2+}]_i$ levels in the control and after BIM-I treatment. *, significant decrease *versus* flow responses in the control ($p < 0.001$).

mated that this maneuver produces shear stress of ~3 dynes/cm^2 (12). This value fits well within the physiological range of shear stress present in the rat and mouse collecting duct as was assessed previously (10, 24). Prior termination of a respective cell-permeable activator/inhibitor of PKC- and PKA-dependent pathways did not affect the magnitude of the flow-mediated $[Ca^{2+}]_i$ response due to poor reversibility of the agent.

Data Analysis—All summarized data are reported as means ± S.E. Data were compared using a *t* test or one-way analysis of variance as appropriate. $p \leq 0.05$ was considered significant.

RESULTS

PKC but Not PKA Cascades Acutely Regulate Flow-dependent $[Ca^{2+}]_i$ Responses in Distal Nephron Cells—We have recently documented that the Ca^{2+}-permeable TRPV4 channel is a critical determinant of mechanosensitive properties in distal nephron cells (10, 12). Genetic deletion of TRPV4 abolishes $[Ca^{2+}]_i$ elevations in response to elevated flow in murine distal nephrons (12). PKC and PKA can directly phosphorylate TRPV4 in expression systems (19). Here, we probed whether these signaling cascades are involved in controlling mechanosensitive $[Ca^{2+}]_i$ elevations by affecting TRPV4 activity and expression patterns in freshly isolated split-opened distal nephrons. Fig. 1*A* documents the average time course of changes in $[Ca^{2+}]_i$ levels in individual cells within a split-opened area of freshly isolated distal nephrons in response to an abrupt 10-fold elevation in flow over the apical surface. Acute stimulation of PKC with 200 nM phorbol 12-myristate 13-acetate (PMA) greatly potentiated flow-mediated elevations in $[Ca^{2+}]_i$. Of note, PMA treatment also had a mild stimulatory effect on the basal levels of $[Ca^{2+}]_i$ (Fig. 1*A*). As summarized in Fig. 1*B*, the responses to flow were similarly increased from 31 ± 3 nM in the control to 49 ± 4 nM and 58 ± 5 nM when PMA was applied for 5 and 15 min, respectively. Administration of a highly selective, cell-permeable PKC inhibitor, bisindolylmaleimide I (BIM-I; 200 nM), for 10 min significantly decreased the amplitude of the flow-mediated $[Ca^{2+}]_i$ response from 32 ± 2 nM to 12 ± 2 nM (Fig. 1, *C* and *D*). Pharmacological PKC inhibition also had a tendency to decrease basal $[Ca^{2+}]_i$ levels (Fig. 1*C*). Overall, we conclude that $[Ca^{2+}]_i$ responses to elevated flow in distal nephron cells are positively regulated by the PKC signaling cascade.

We next probed the involvement of the PKA signaling cascade in the regulation of flow-dependent Ca^{2+} responses in distal nephron cells. Fig. 2*A* documents the average time course of changes in $[Ca^{2+}]_i$ levels in response to elevated flow under

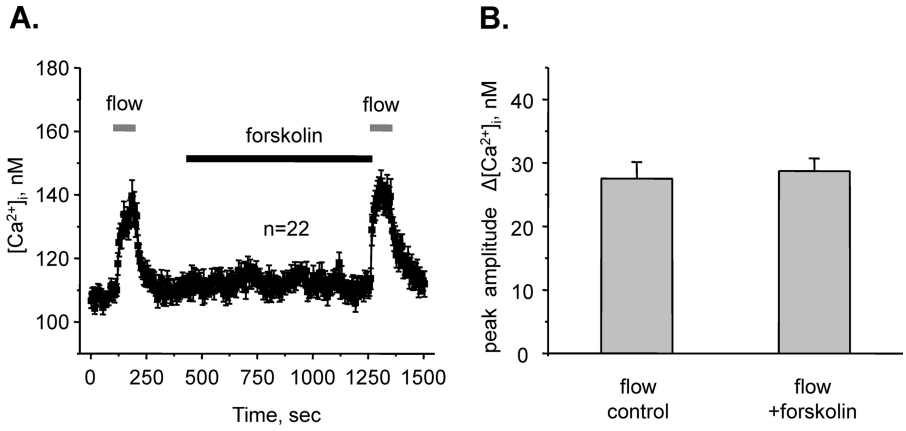

FIGURE 2. **Acute stimulation of the PKA-dependent pathway does not affect mechanosensitive $[Ca^{2+}]_i$ elevations in distal nephron cells.** *A*, average time course of changes in $[Ca^{2+}]_i$ levels in response to 10-fold elevations in flow over the apical surface (*gray bars*) for individual distal nephron cells in the control and after treatment with 20 μM forskolin (*black bar*). *B*, summary graph of the flow-induced changes in $[Ca^{2+}]_i$ levels in the control and after forskolin.

the control conditions and after 15 min treatment with forskolin (20 μM) to elevate intracellular cAMP levels. However, this maneuver failed to affect flow-induced Ca^{2+} responses in distal nephron cells. The amplitudes of the response were 28 ± 3 nM and 29 ± 3 nM in the control and after forskolin treatment, respectively (Fig. 2*B*). These results suggest that acute activation of the PKA signaling cascade alone has no appreciable role in the regulation of TRPV4 functional activity and, subsequently, flow-dependent $[Ca^{2+}]_i$ elevations in distal nephron cells.

TRPV4 Trafficking Is Regulated by PKA but Not PKC—We next used immunofluorescence microscopy in split-opened distal nephrons to examine whether stimulation of the PKC and PKA cascades alters subcellular TRPV4 localization to promote trafficking to the apical plasma membrane. Consistent with our previous report (12), TRPV4 expression was dominant in the apical/subapical regions under the control conditions, as apparent from a representative confocal fluorescent image in Fig. 3*A*. Pretreatment with the PKC activator PMA (200 nM) for 15 min had no apparent effect on TRPV4 subcellular localization (Fig. 3*B*). In contrast, TRPV4 localized to the apical plasma membrane when split-opened distal nephrons were pretreated with 20 μM forskolin for 15 min (Fig. 3*C*). Forskolin-induced redistribution was precluded by the PKA inhibitor H-89 (20 μM) (Fig. 3*D*).

To perform a quantitative estimation of the observed changes in subcellular TRPV4 localization, we employed line-scan analysis of the fluorescent signal distribution along the *z*-axis in cross-sections of three-dimensional stacks similar to those shown in Fig. 3. Fig. 4*A* shows the averaged distribution pattern of fluorescence intensity representing TRPV4 localization in the control and after pretreatment with PMA, forskolin, and forskolin and H-89. As is clear, stimulation of the PKA pathway with forskolin shifted the maximum of the fluorescent signal toward the apical region. Furthermore, forskolin also caused sharpening of the fluorescence intensity profile. As summarized in Fig. 4*B*, the average half-width of the fluorescence intensity was significantly reduced from 3.06 ± 0.07 μm (n = 108) in the control to 1.34 ± 0.04 μm (n = 123) after forskolin treatment. At the same time, the half-width was 2.92 ± 0.17 μm (n = 105) after treatment with PMA and 2.99 ± 0.18 μm (n = 95) after treatment with H-89 and forskolin. These values were not significantly different from the control. Overall, the results in Figs. 3 and 4 suggest that activation of PKA but not PKC signaling cascades promotes TRPV4 trafficking to the apical plasma membrane.

The apparent lack of forskolin-mediated augmentation of the flow-induced $[Ca^{2+}]_i$ response (Fig. 2), despite the prominent trafficking of TRPV4 to the apical compartment (Figs. 3 and 4), may indicate that translocated channels were not yet inserted into the plasma membrane. In this case, $[Ca^{2+}]_i$ stimulation was required to incorporate TRPV4 into the apical membrane and augment cellular responses to elevated flow. To probe this, we treated split-opened distal nephrons with 20 μM forskolin and quantified the amplitudes of two consequent flow-induced $[Ca^{2+}]_i$ responses in the continued presence of the PKA cascade activator (Fig. 5*A*). However, $[Ca^{2+}]_i$ elevations induced by the first application of increased flow did not result in appreciable potentiation of the second flow-mediated $[Ca^{2+}]_i$ response. As summarized in Fig. 5*B*, the amplitudes of the first and second responses during forskolin treatment were 27 ± 1 and 25 ± 1 nM, respectively, and were not different from the amplitude of the flow-mediated $[Ca^{2+}]_i$ response in the control (29 ± 2 nM). Therefore, it appears that activation of the PKA-dependent pathway likely results in translocation of silent TRPV4 to the apical membrane and that lack of augmentation of flow-dependent $[Ca^{2+}]_i$ responses is not associated with inability of the channels to be inserted.

Coordinated Actions of the PKC and PKA Cascades on Flow-mediated $[Ca^{2+}]_i$ Elevations in the Distal Nephron—Our results point to distinct modes of TRPV4 regulation by PKC and PKA signaling cascades. Whereas the PKC-dependent pathway stimulated TRPV4 and enhanced mechanosensitive $[Ca^{2+}]_i$ responses (Fig. 1) without affecting subcellular TRPV4 distribution (Fig. 3*B*), the PKA-dependent pathway promoted apical TRPV4 trafficking (Fig. 3*C*) but failed to augment functional TRPV4 status (Figs. 2 and 5). Thus, we next tested whether PKA- and PKC-dependent pathways are cooperative in augmenting TRPV4-mediated $[Ca^{2+}]_i$ responses to flow. Concomitant stimulation of both pathways with 200 nM PMA

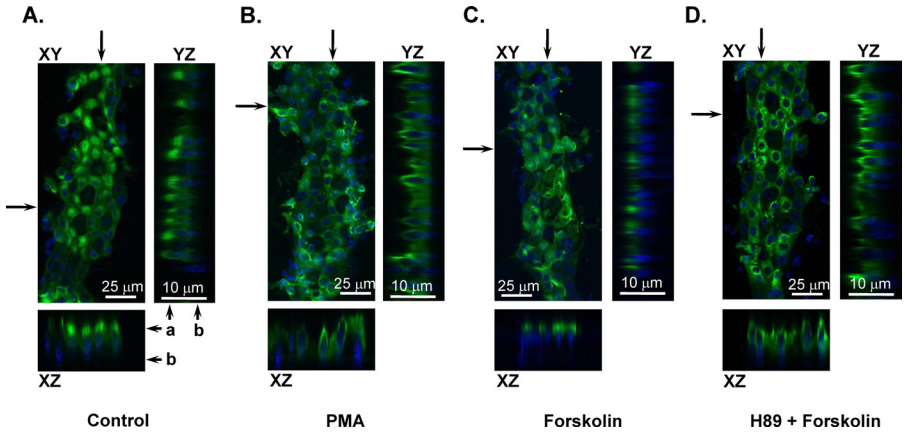

FIGURE 3. **Distinct effects of PKC- and PKA-dependent signaling cascades on subcellular TRPV4 localization in distal nephron cells.** Shown are representative confocal plane micrographs (axes are shown) and corresponding cross-sections (indicated by *arrows*) demonstrating TRPV4 localization (anti-TRPV4, pseudocolor *green*) in split-opened murine distal nephrons in the control (*A*) and after a 15-min pretreatment with 200 nM PMA (*B*), a 15-min pretreatment with 20 μM forskolin (*C*), and a 15-min pretreatment with 20 μM forskolin and 20 μM H-89 (*D*). Nuclear DAPI staining is shown by pseudocolor *blue*. *a* and *b* indicate the apical and basolateral sides, respectively.

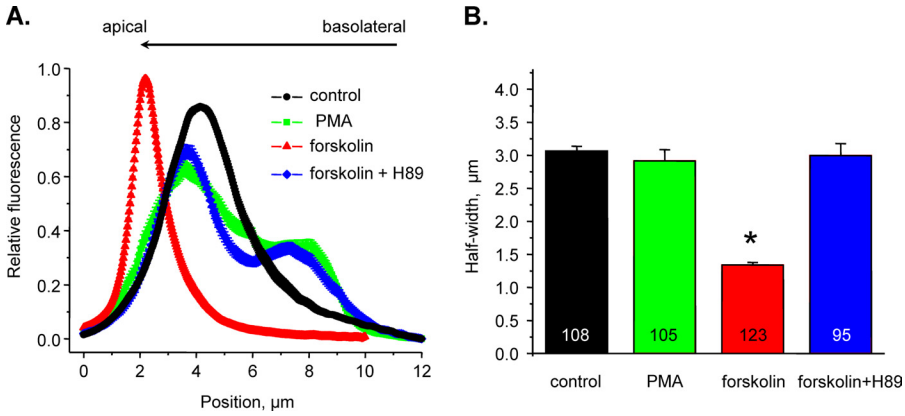

FIGURE 4. **Acute activation of the PKA signaling cascade promotes apical TRPV4 translocation.** *A*, distribution of averaged relative fluorescent signals representing TRPV4 localization along a line on *z*-axis in individual cells from distal nephrons similar to that shown in Fig. 3 in the control (*black*) and after a 15-min pretreatment with 200 nM PMA (*green*), a 15-min pretreatment with 20 μM forskolin (*red*), and a 15-min pretreatment with 20 μM forskolin and 20 μM H-89 (*blue*). For each individual cell, the fluorescent signals were normalized to their corresponding maximal value. The positions of the apical and basolateral sides are shown by the *arrow* at the top. *B*, summary graph of half-width means for distributions of fluorescent signals shown in *A*. *, significant decrease *versus* control ($p < 0.001$).

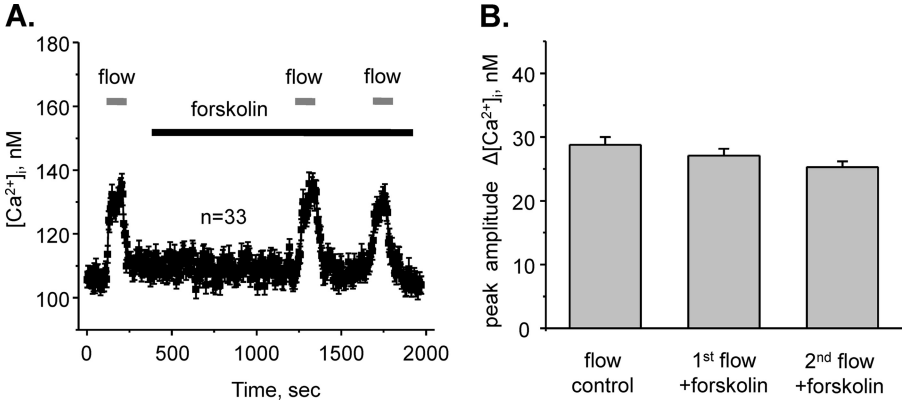

FIGURE 5. **Elevations in $[Ca^{2+}]_i$ do not lead to augmentation of flow-mediated responses during stimulation of the PKA cascade.** *A*, average time course of changes in $[Ca^{2+}]_i$ levels in response to a 10-fold elevation in flow over the apical surface in the control and two repetitive flow stimulations (*gray bars*) after treatment with 20 μM forskolin (*black bar*). *B*, summary graph of the respective flow-induced changes in $[Ca^{2+}]_i$ levels in the control and after forskolin as demonstrated in *A*.

and 20 μM forskolin drastically augmented the amplitude of flow-induced $[Ca^{2+}]_i$ responses (Fig. 6*A*, *black trace*). This elevation was significantly greater than that in response to application of PMA alone (Fig. 6*A*, *gray trace*). The absolute elevations in $[Ca^{2+}]_i$ in response to flow were 34 ± 2, 77 ± 4, and 55 ± 3 nM in the control, after treatment with PMA + forskolin, and after treatment with PMA alone, respectively (Fig. 6*B*). Interestingly, we observed a prominent gradual increase of ~80

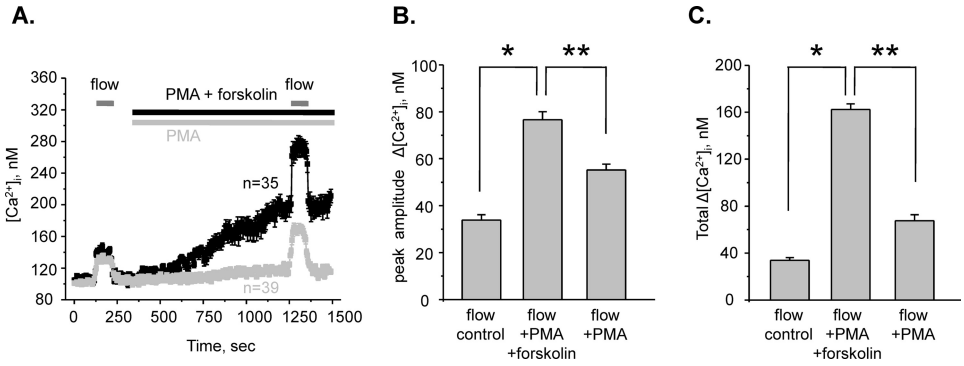

FIGURE 6. **Concomitant activation of PKC and PKA cascades additively augments flow-dependent $[Ca^{2+}]_i$ responses and increases basal $[Ca^{2+}]_i$ levels in distal nephron cells.** *A*, average time course of $[Ca^{2+}]_i$ changes in individual distal nephron cells (*black trace*) in response to abrupt 10-fold elevations in flow from the apical side (*gray bars*) for individual distal nephron cells in the control and after treatment with 200 nM PMA and 20 μM forskolin (*black bar*). For comparison, the average time course of $[Ca^{2+}]_i$ changes in individual distal nephron cells (*gray trace*) in response to elevated flow in the control and after treatment with 200 nM PMA (*gray bar*) is also shown. *B*, summary graph of the amplitude of flow-induced $[Ca^{2+}]_i$ elevations in the control, after application of PMA and forskolin, and after application of PMA alone. *C*, summary graph of the absolute changes in $[Ca^{2+}]_i$ from the initial base-line levels during elevated flow in the control, after application of PMA and forskolin, and after application of PMA alone. *, significant increase *versus* flow responses in the control ($p < 0.001$); **, significant increase *versus* flow and PMA ($p < 0.001$).

nM in basal $[Ca^{2+}]_i$ levels in distal nephron cells upon concomitant treatment with 200 nM PMA and 20 μM forskolin (Fig. 6*A*). Therefore, the absolute elevation of $[Ca^{2+}]_i$ from the values under unstimulated conditions reflects the total level of TRPV4 activation by mechanical stimuli (*i.e.* flow) in the presence of simultaneous stimulation of the PKA and PKC cascades. As summarized in Fig. 6*C*, the absolute amplitude of the $[Ca^{2+}]_i$ response to flow was 162 $\pm$ 5 nM, which was significantly greater than the response in the presence of PKC stimulation alone (68 $\pm$ 5 nM).

Finally, to probe whether the additive stimulation of the flow-dependent $[Ca^{2+}]_i$ response and gradual increases in the basal $[Ca^{2+}]_i$ levels in response to simultaneous activation of the PKC and PKA cascades occur in a TRPV4-dependent manner, we repeated the treatment with PMA and forskolin in the presence of the selective TRPV4 inhibitor HC-067047 (4 μM). As is clear from the average time course (Fig. 7*A*), TRPV4 blockade abolished the progressive increase in $[Ca^{2+}]_i$ levels. Moreover, HC-067047 precluded flow-mediated $[Ca^{2+}]_i$ responses even in the presence of the activated PKC and PKA cascades (Fig. 7*B*). The amplitudes of the flow-mediated $[Ca^{2+}]_i$ response were 33 $\pm$ 2 nM in the control and 5 $\pm$ 2 nM after treatment with forskolin, PMA, and HC-067047. Overall, we conclude that the coordinated stimulation of both PKC and PKA cascades additively increases the amplitude of the TRPV4-mediated $[Ca^{2+}]_i$ response to flow and, importantly, augments the basal TRPV4 activity, resulting in a progressive increase in the resting $[Ca^{2+}]_i$ levels.

DISCUSSION

It has been recently demonstrated that the activity of the Ca^{2+}-permeable TRPV4 channel is central for $[Ca^{2+}]_i$ elevations in distal nephron cells in response to dynamic changes in tubular fluid flow (11, 12, 16, 20). Adequate mechanosensitive $[Ca^{2+}]_i$ responses are important determinants of many physiological processes in late nephron segments, including flow-dependent K^+ secretion (15, 25), regulatory volume decreases (26), etc. Furthermore, we and others have recently demonstrated that pharmacological stimulation of TRPV4 activity is instrumental for blunting renal cystogenesis in ARPKD models (18, 27). In this study, we defined two distinct intracellular signaling cascades separately controlling TRPV4 trafficking and functional activity in murine distal nephrons. We found that the PKC-dependent signaling pathway is responsible for augmented TRPV4 activation by elevated flow over the apical plasma membrane. In contrast, TRPV4 translocation to the apical plasma membrane is a PKA-dependent process.

We have provided substantial experimental evidence that TRPV4 serves as a route of Ca^{2+} influx into distal nephron cells in response to elevated luminal flow. First, we documented that silencing of TRPV4 expression in cultured collecting duct cells disrupts Ca^{2+} responses to shear stress (10). Second, genetic ablation of TRPV4 in mice abolishes flow-induced $[Ca^{2+}]_i$ elevations in the connecting tubule and cortical collecting duct (12). Consistently, in this study, we have demonstrated that pharmacological inhibition of TRPV4 with the highly selective antagonist HC-067047 precludes changes in $[Ca^{2+}]_i$ during elevations in flow (Fig. 7). Finally, we and others found that the presence of extracellular Ca^{2+} is mandatory for flow-induced $[Ca^{2+}]_i$ elevations in renal cells (10, 28). Therefore, we are confident that monitoring changes in $[Ca^{2+}]_i$ in freshly isolated split-opened murine distal nephrons is a reliable way to assess the rate of TRPV4 activation in native tissue by a physiologically relevant stimulus, *i.e.* elevated flow. In this study, we did not identify principal and intercalated cells. As we reported previously (12), principal cells exhibit a mildly increased amplitude of flow-mediated $[Ca^{2+}]_i$ responses compared with intercalated cells, and this correlates with higher levels of TRPV4 expression in the former. A similar amplitude of flow-induced increases in $[Ca^{2+}]_i$ in principal and intercalated cells was also reported in microperfused rabbit cortical collecting ducts (29, 30). The detailed analysis did not reveal noticeable heterogeneity in the rate of potentiation of flow-dependent $[Ca^{2+}]_i$ responses in individual cells during activation of PKC signaling with PMA (Fig. 1). Furthermore, we have also observed similar translocation of TRPV4 to the apical membrane in "low TRPV4-expressing" intercalated cells after treatment with for-

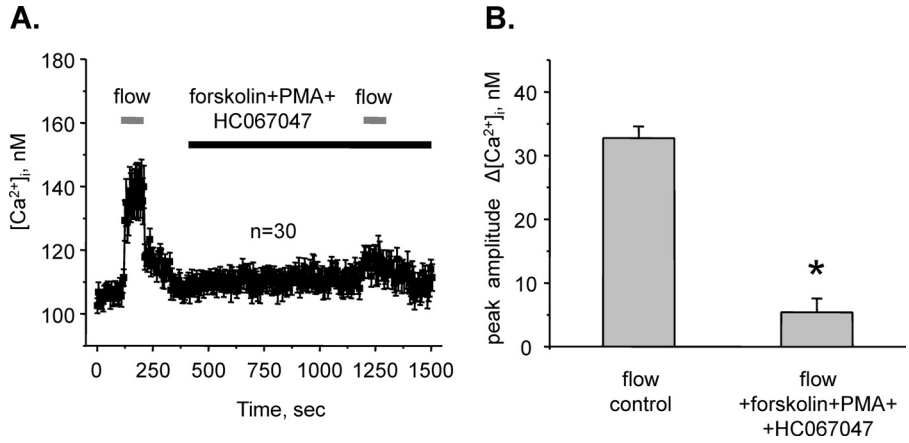

FIGURE 7. **Regulation of mechanosensitive $[Ca^{2+}]_i$ responses by PKA and PKC cascades occurs in a TRPV4-dependent manner.** *A*, average time course of changes in $[Ca^{2+}]_i$ levels in response to a 10-fold elevation in flow over the apical surface (*gray bars*) for individual distal nephron cells in the control and after combined treatment with 200 nM PMA, 20 μM forskolin, and the selective TRPV4 inhibitor HC-067047 (4 μM). *B*, summary graph of the flow-induced changes in $[Ca^{2+}]_i$ levels in the control and after treatment with PMA, forskolin, and HC-067047. *, significant decrease *versus* flow responses in the control ($p < 0.001$).

skolin (Fig. 3). Thus, it is reasonable to suggest that the mechanisms of TRPV4 regulation by PKA and PKC in principal and intercalated cells are the same.

We have shown that flow-induced $[Ca^{2+}]_i$ elevations are under dynamic regulation of the PKC-dependent pathway. Stimulation of PKC led to an acute augmentation of $[Ca^{2+}]_i$ responses to elevated flow (Fig. 1, *A* and *B*), whereas inhibition of PKC with BIM-I greatly diminished mechanosensitive $[Ca^{2+}]_i$ elevations (Fig. 1, *C* and *D*). Importantly, we demonstrated that this regulation occurred in a TRPV4-dependent manner because inhibition of TRPV4 with HC-067047 abolished cellular responses to elevated flow even upon activation of PKC (Fig. 7). Interestingly, inhibition of PKC with BIM-I and Go6976 was shown to preclude transient flow-mediated $[Ca^{2+}]_i$ elevations and flow-dependent potassium secretion in perfused rabbit cortical collecting ducts (30). In contrast, we did not observe complete inhibition of flow-mediated $[Ca^{2+}]_i$ responses during PKC blockade. However, we used a 5-fold lower concentration of BIM-I, which is more selective. PKC was shown to directly phosphorylate multiple Ser/Thr residues within the N terminus of TRPV4 overexpressed in HEK293 cells to augment channel activation by hypotonicity (19). It remains to be determined whether PKC-mediated regulation of TRPV4 function in distal nephron cells involves direct channel phosphorylation. Of note, PMA can also directly interact with transmembrane domains 3 and 4 of TRPV4 (31, 32). However, this can lead to activation of the channel only at 37 °C and has a minor direct effect on TRPV4 activity at room temperature as used here.

The important observation of this study is that stimulation of TRPV4 trafficking to the apical plasma membrane is not associated with augmentation of TRPV4-mediated $[Ca^{2+}]_i$ responses to elevated flow (Figs. 2–4). Furthermore, we have demonstrated that translocation of TRPV4 to the apical plasma membrane is regulated by PKA-dependent mechanisms (Fig. 4). This indicates that TRPV4 trafficking in distal nephron cells might be at least partially under the control of antidiuretic hormone (vasopressin). TRPV4 was recently shown to functionally interact with AQP2, the well known end effector of vasopressin, and the trafficking of TRPV4 to the plasma membrane in M1 collecting duct cells occurs only in the presence of AQP2 (26). Although this was associated with enhanced responses to hypotonicity, we failed to observe an augmented response to flow in forskolin-treated distal nephrons (Fig. 2). The nature of this discrepancy requires further investigation. Importantly, lack of mechanosensitive $[Ca^{2+}]_i$ responses (33–35) and elevated cAMP levels (36, 37) have been consistently reported for cyst cells of many polycystic kidney disease models. Using a novel preparation to isolate collecting duct-derived cyst monolayers from a rat model of ARPKD, we recently demonstrated drastic decreases in TRPV4 activity despite prominent apical localization of the channel in cyst cells, which is likely a consequence of elevated cAMP levels (18). This is consistent with our conclusions that trafficking and activation of TRPV4 require distinct intracellular signaling inputs. Interestingly, another Ca^{2+}-permeable channel, TRPC3, which is natively expressed in distal nephron cells (38), is also translocated to the apical plasma membrane in response to vasopressin treatment via stimulation of the cAMP/PKA pathway (39, 40). However, it remains unclear whether this redistribution is associated with augmented TRPC3-dependent $[Ca^{2+}]_i$ elevations.

In this study, we have also provided evidence that TRPV4 activity is an important determinant of basal $[Ca^{2+}]_i$ levels in distal nephron cells. Stimulation of PKC led not only to augmentation of TRPV4-mediated $[Ca^{2+}]_i$ responses to flow but also to a gradual elevation of the $[Ca^{2+}]_i$ base line (Fig. 1*A*). This elevation was greatly potentiated after stimulation of apical TRPV4 trafficking with PKA (Fig. 6*A*). In contrast, we observed a tendency to reduce basal $[Ca^{2+}]_i$ levels when PKC was inhibited by BIM-I (Fig. 1*C*). These observations support the conception that basal TRPV4 activity under unstimulated conditions (*i.e.* in the absence of external mechanical inputs) is sufficient to adjust resting $[Ca^{2+}]_i$ levels in murine distal nephron cells. We recently reported that impaired TRPV4 activity is associated with reduced resting $[Ca^{2+}]_i$ levels in collecting duct-derived cyst cells during ARPKD and, vice versa, that restoration of TRPV4 activity increases $[Ca^{2+}]_i$ levels to the values seen in normal rat distal nephron cells (18).

In summary, in this study, we have identified the signaling determinants of TRPV4 function in murine native distal

nephron cells. We have reported that stimulation of TRPV4 activity and TRPV4 trafficking is under discrete but synergistic control of the PKC- and PKA-dependent pathways. This enables the system to manipulate resting $[Ca^{2+}]_i$ levels as well as to regulate the magnitude of $[Ca^{2+}]_i$ responses to dynamic changes in tubular flow. However, the upstream physiological stimuli controlling TRPV4-based mechanosensitive $[Ca^{2+}]_i$ responses to regulate transport rates in the distal nephron have yet to be established.

REFERENCES

1. Venkatachalam, K., and Montell, C. (2007) TRP channels. *Annu. Rev. Biochem.* **76,** 387–417
2. Nilius, B., and Owsianik, G. (2011) The transient receptor potential family of ion channels. *Genome Biol.* **12,** 218
3. Nilius, B., Owsianik, G., Voets, T., and Peters, J. A. (2007) Transient receptor potential cation channels in disease. *Physiol. Rev.* **87,** 165–217
4. Nilius, B., and Owsianik, G. (2010) Transient receptor potential channelopathies. *Pflugers Arch.* **460,** 437–450
5. Dietrich, A., Chubanov, V., and Gudermann, T. (2010) Renal TRPathies. *J. Am. Soc. Nephrol.* **21,** 736–744
6. Woudenberg-Vrenken, T. E., Bindels, R. J., and Hoenderop, J. G. (2009) The role of transient receptor potential channels in kidney disease. *Nat. Rev. Nephrol.* **5,** 441–449
7. Nilius, B., and Voets, T. (2013) The puzzle of TRPV4 channelopathies. *EMBO Rep.* **14,** 152–163
8. Everaerts, W., Nilius, B., and Owsianik, G. (2010) The vanilloid transient receptor potential channel TRPV4: from structure to disease. *Prog. Biophys. Mol. Biol.* **103,** 2–17
9. Nilius, B., Vriens, J., Prenen, J., Droogmans, G., and Voets, T. (2004) TRPV4 calcium entry channel: a paradigm for gating diversity. *Am. J. Physiol. Cell Physiol.* **286,** C195–C205
10. Wu, L., Gao, X., Brown, R. C., Heller, S., and O'Neil, R. G. (2007) Dual role of the TRPV4 channel as a sensor of flow and osmolality in renal epithelial cells. *Am. J. Physiol. Renal Physiol.* **293,** F1699–F1713
11. Pochynyuk, O., Zaika, O., O'Neil, R. G., and Mamenko, M. (2013) Novel insights into TRPV4 function in the kidney. *Pflugers Arch.* **465,** 177–186
12. Berrout, J., Jin, M., Mamenko, M., Zaika, O., Pochynyuk, O., and O'Neil, R. G. (2012) Function of TRPV4 as a mechanical transducer in flow-sensitive segments of the renal collecting duct system. *J. Biol. Chem.* **287,** 8782–8791
13. Liu, W., Morimoto, T., Woda, C., Kleyman, T. R., and Satlin, L. M. (2007) Ca^{2+} dependence of flow-stimulated K secretion in the mammalian cortical collecting duct. *Am. J. Physiol. Renal Physiol.* **293,** F227–F235
14. Pluznick, J. L., and Sansom, S. C. (2006) BK channels in the kidney: role in K^+ secretion and localization of molecular components. *Am. J. Physiol. Renal Physiol.* **291,** F517–F529
15. Taniguchi, J., Tsuruoka, S., Mizuno, A., Sato, J., Fujimura, A., and Suzuki, M. (2007) TRPV4 as a flow sensor in flow-dependent K^+ secretion from the cortical collecting duct. *Am. J. Physiol. Renal Physiol.* **292,** F667–F673
16. Köttgen, M., Buchholz, B., Garcia-Gonzalez, M. A., Kotsis, F., Fu, X., Doerken, M., Boehlke, C., Steffl, D., Tauber, R., Wegierski, T., Nitschke, R., Suzuki, M., Kramer-Zucker, A., Germino, G. G., Watnick, T., Prenen, J., Nilius, B., Kuehn, E. W., and Walz, G. (2008) TRPP2 and TRPV4 form a polymodal sensory channel complex. *J. Cell Biol.* **182,** 437–447
17. Du, J., Wong, W. Y., Sun, L., Huang, Y., and Yao, X. (2012) Protein kinase G inhibits flow-induced Ca^{2+} entry into collecting duct cells. *J. Am. Soc. Nephrol.* **23,** 1172–1180
18. Zaika, O., Mamenko, M., Berrout, J., Boukelmoune, N., O'Neil, R. G., and Pochynyuk, O. (2013) TRPV4 dysfunction promotes renal cystogenesis in autosomal recessive polycystic kidney disease. *J. Am. Soc. Nephrol.* **24,** 604–616
19. Fan, H. C., Zhang, X., and McNaughton, P. A. (2009) Activation of the TRPV4 ion channel is enhanced by phosphorylation. *J. Biol. Chem.* **284,** 27884–27891
20. Mamenko, M., Zaika, O., Jin, M., O'Neil, R. G., and Pochynyuk, O. (2011) Purinergic activation of Ca-permeable TRPV4 channels is essential for mechano-sensitivity in the aldosterone-sensitive distal nephron. *PLoS. One* **6,** e22824
21. Mamenko, M., Zaika, O., Ilatovskaya, D. V., Staruschenko, A., and Pochynyuk, O. (2012) Angiotensin II increases activity of the epithelial Na^+ channel (ENaC) in distal nephron additively to aldosterone. *J. Biol. Chem.* **287,** 660–671
22. Mamenko, M., Zaika, O., Doris, P. A., and Pochynyuk, O. (2012) Salt-dependent inhibition of epithelial Na^+ channel-mediated sodium reabsorption in the aldosterone-sensitive distal nephron by bradykinin. *Hypertension* **60,** 1234–1241
23. Zaika, O., Mamenko, M., O'Neil, R. G., and Pochynyuk, O. (2011) Bradykinin acutely inhibits activity of the epithelial Na^+ channel in mammalian aldosterone-sensitive distal nephron. *Am. J. Physiol. Renal Physiol.* **300,** F1105–F1115
24. Cai, Z., Xin, J., Pollock, D. M., and Pollock, J. S. (2000) Shear stress-mediated NO production in inner medullary collecting duct cells. *Am. J. Physiol. Renal Physiol.* **279,** F270–F274
25. Taniguchi, J., and Imai, M. (1998) Flow-dependent activation of maxi K^+ channels in apical membrane of rabbit connecting tubule. *J. Membr. Biol.* **164,** 35–45
26. Galizia, L., Pizzoni, A., Fernandez, J., Rivarola, V., Capurro, C., and Ford, P. (2012) Functional interaction between AQP2 and TRPV4 in renal cells. *J. Cell. Biochem.* **113,** 580–589
27. Gradilone, S. A., Masyuk, T. V., Huang, B. Q., Banales, J. M., Lehmann, G. L., Radtke, B. N., Stroope, A., Masyuk, A. I., Splinter, P. L., and LaRusso, N. F. (2010) Activation of Trpv4 reduces the hyperproliferative phenotype of cystic cholangiocytes from an animal model of ARPKD. *Gastroenterology* **139,** 304–314.e2
28. Nauli, S. M., Alenghat, F. J., Luo, Y., Williams, E., Vassilev, P., Li, X., Elia, A. E., Lu, W., Brown, E. M., Quinn, S. J., Ingber, D. E., and Zhou, J. (2003) Polycystins 1 and 2 mediate mechanosensation in the primary cilium of kidney cells. *Nat. Genet.* **33,** 129–137
29. Woda, C. B., Leite, M., Jr., Rohatgi, R., and Satlin, L. M. (2002) Effects of luminal flow and nucleotides on $[Ca^{2+}]_i$ in rabbit cortical collecting duct. *Am. J. Physiol. Renal Physiol.* **283,** F437–F446
30. Liu, W., Wei, Y., Sun, P., Wang, W. H., Kleyman, T. R., and Satlin, L. M. (2009) Mechanoregulation of BK channel activity in the mammalian cortical collecting duct: role of protein kinases A and C. *Am. J. Physiol. Renal Physiol.* **297,** F904–F915
31. Gao, X., Wu, L., and O'Neil, R. G. (2003) Temperature-modulated diversity of TRPV4 channel gating: activation by physical stresses and phorbol ester derivatives through protein kinase C-dependent and -independent pathways. *J. Biol. Chem.* **278,** 27129–27137
32. Vriens, J., Owsianik, G., Janssens, A., Voets, T., and Nilius, B. (2007) Determinants of 4α-phorbol sensitivity in transmembrane domains 3 and 4 of the cation channel TRPV4. *J. Biol. Chem.* **282,** 12796–12803
33. Xu, C., Shmukler, B. E., Nishimura, K., Kaczmarek, E., Rossetti, S., Harris, P. C., Wandinger-Ness, A., Bacallao, R. L., and Alper, S. L. (2009) Attenuated, flow-induced ATP release contributes to absence of flow-sensitive, purinergic Ca_i^{2+} signaling in human ADPKD cyst epithelial cells. *Am. J. Physiol. Renal Physiol.* **296,** F1464–F1476
34. Hovater, M. B., Olteanu, D., Hanson, E. L., Cheng, N. L., Siroky, B., Fintha, A., Komlosi, P., Liu, W., Satlin, L. M., Bell, P. D., Yoder, B. K., and Schwiebert, E. M. (2008) Loss of apical monocilia on collecting duct principal cells impairs ATP secretion across the apical cell surface and ATP-dependent and flow-induced calcium signals. *Purinergic Signal.* **4,** 155–170
35. Siroky, B. J., Ferguson, W. B., Fuson, A. L., Xie, Y., Fintha, A., Komlosi, P., Yoder, B. K., Schwiebert, E. M., Guay-Woodford, L. M., and Bell, P. D. (2006) Loss of primary cilia results in deregulated and unabated apical calcium entry in ARPKD collecting duct cells. *Am. J. Physiol. Renal Physiol.* **290,** F1320–F1328
36. Gattone, V. H., 2nd, Wang, X., Harris, P. C., and Torres, V. E. (2003) Inhibition of renal cystic disease development and progression by a vasopressin V2 receptor antagonist. *Nat. Med.* **9,** 1323–1326
37. Yamaguchi, T., Nagao, S., Kasahara, M., Takahashi, H., and Grantham, J. J. (1997) Renal accumulation and excretion of cyclic adenosine monophosphate in a murine model of slowly progressive polycystic kidney disease.

Am. J. Kidney Dis. **30,** 703–709
38. Goel, M., Sinkins, W. G., Zuo, C. D., Estacion, M., and Schilling, W. P. (2006) Identification and localization of TRPC channels in the rat kidney. *Am. J. Physiol. Renal Physiol.* **290,** F1241–F1252
39. Goel, M., Sinkins, W. G., Zuo, C. D., Hopfer, U., and Schilling, W. P. (2007) Vasopressin-induced membrane trafficking of TRPC3 and AQP2 channels in cells of the rat renal collecting duct. *Am. J. Physiol. Renal Physiol.* **293,** F1476–F1488
40. Goel, M., Zuo, C. D., and Schilling, W. P. (2010) Role of cAMP/PKA signaling cascade in vasopressin-induced trafficking of TRPC3 channels in principal cells of the collecting duct. *Am. J. Physiol. Renal Physiol.* **298,** F988–F996